

SOLUTION MINING RESEARCH INSTITUTE

105 Apple Valley Circle
Clarks Summit, PA 18411, USA

Telephone: +1 570-585-8092

Fax: +1 505-585-8091

www.solutionmining.org

Technical
Conference
Paper



Experimental Deformation of Salt in Cyclic Loading, Insights from Acoustic Emission Measurements

Stephen Bauer, Scott Broome, David Bronowski, Alex Rinehart¹, Mathew D. Ingraham²

Sandia National Laboratories, Albuquerque, New Mexico, USA

¹**New Mexico Tech, Socorro, New Mexico, USA**

²**Clarkson University, Potsdam, New York, USA**

SMRI Spring 2011 Technical Conference
18-19 April 2011
Galveston, Texas, USA

EXPERIMENTAL DEFORMATION OF SALT IN CYCLIC LOADING INSIGHTS FROM ACOUSTIC EMISSION MEASUREMENTS

Stephen Bauer, Scott Broome, David Bronowski, Alex Rinehart¹ and Mathew Ingraham²

Sandia National Laboratories*, Albuquerque, New Mexico, USA

¹New Mexico Tech, Socorro, New Mexico, USA

²Clarkson University, Potsdam, New York, USA

Abstract

Compressed air energy storage (CAES) in geologic media has been proposed to help ensure reliability of renewable energy sources, for example wind and solar, by providing a means to store energy when excess energy was available, and to provide an energy source during non productive renewable energy time periods. Such a storage media may experience hourly (perhaps small) pressure swings within a geologic storage media. This implies that the storage “container”, for example, a salt cavern, may experience small irregular pressure cycling.

An ongoing study is underway wherein confined rock salt specimens (a Gulf Coast domal salt 98% halite) have been cyclically stressed. The rock salt was first characterized by developing a dilatancy criterion. Then, specimens confined at 3000 psi were cycled (in triaxial compression) between 25-30% and 50-60% of the dilatant strength. Specimens were cycled up to the 50-60% load, held at constant stress for ~ 3 hours, then cycled down to the 25-30% load, and again held for 3 hours. Specimens experienced about four load cycles per day; tests ran from 12 days to about 60 days, resulting in about 40 to 240 load cycles on different specimens. Acoustic emission (AE) detection during these cyclic creep tests provides insight into when microcrack damage occurs during the complicated deformation history. AEs were detected during the constant stress portions of the test at both the upper and lower test load level.

Also during these tests, axial and radial displacements were recorded as well. It was found that Young's Modulus determined from unloading cycles decreased with increasing axial strain, load cycle, and time after an initial period of limited change. Using a dilatancy criterion of the volume strain changing from compaction to dilation, the specimens are also observed to dilate at these low stress levels. These strain measurements, together with AE measurements indicate that the specimens are cracking at these low cyclically-applied differential stresses well below the short-term testing dilation criterion curve.

The cyclic testing has been augmented by constant mean stress and constant strain rate testing in which AE measurements were recorded. These additional tests provide insight into the semi-brittle deformation of salt during application and hold of confining pressure, monotonic loading, and decreases in confining pressure after deformation.

Key words: Cyclic loading, Rock salt, Semi-brittle Deformation, Renewable Energy, Rock Mechanics

*Sandia National Laboratories is a multi-program laboratory managed and operated by Sandia Corporation, a wholly owned subsidiary of Lockheed Martin Corporation, for the U.S. Department of Energy's National Nuclear Security Administration under contract DE-AC04-94AL85000.

Introduction

The U.S. administration's energy and environment agenda calls for substantial, near-term increases in renewable energy generation. At the same time, system operators, DOE and other stakeholders are recognizing that the previously existing "reserve capacity" in some energy regions and sub regions has already been committed to support interconnection of the first wave of intermittent renewable generation. In those regions, the critical levels of remaining reserve capacity have already started to slow or preclude the interconnection of the desired next wave of intermittent renewable generation. As a result, developers of new intermittent renewable generation are being required to demonstrate the availability of sufficient back-up generation (typically gas-fired) to firm deliveries of power from their project before they are allowed to interconnect.

Solar power is a predictably intermittent energy source, meaning that although solar power is not available at all times, we can predict generally when it will and will not be available (on a daily basis). Some technologies, such as solar thermal concentrators have an element of thermal storage, such as molten salts. These store spare solar energy in the form of heat which is made available overnight or during periods that solar power is not available to produce electricity. On a day with intermittent clouds passing, for example, power generation from a large photovoltaic array is unpredictable.

Electricity generated from wind power can be highly variable at several different timescales: from hour to hour, daily, and seasonally. Annual variation also exists, but is not as significant. Related to variability is the short-term (hourly or daily) predictability of wind plant output. Like other electricity sources, wind energy must be "scheduled". Wind power forecasting methods are used, but predictability of wind plant output remains low for short-term operation. The first generations of wind power systems have been able to depend on existing peaker capacity to even out their variability, but this is neither a scalable economic solution nor a CO₂ sensible solution.

Renewable power can be supplemented by storage or replaced by other power stations during low renewable generation periods. Transmission networks must already cope with outages of generation plant and daily changes in electrical demand. Systems with large renewable components may need more spinning reserve that is, plants operating at less than full load.

Grid scale energy storage can store energy developed by renewables and release it when needed. Stored energy could increase the economic value of renewable energy since it can be shifted to displace higher cost generation during peak demand periods. Storage can provide reliability without additional transmission costs. There will be generation, transmission, and distribution applications for different storage technologies to support the integration of renewables for both grid performance and grid efficiency.

The addition of utility scale, bulk energy storage will be required to realize the potential of the emerging smart grid and facilitate the integration of additional intermittent renewable generation. Perhaps CAES facilities utilizing the geographically dispersed U.S. salt structures currently offer the greatest potential for additional bulk energy storage.

An experimental and analysis program is underway to help understand the potential for high frequency pressure cycling in underground storage media that may be required to support integration of intermittent renewable generation into the grid. The calculated geomechanical stresses on salt caverns will in part be used to design tests to determine the geomechanical response of cyclically-deformed rock salt. The observed experimental results (damage, dilatancy, healing, and creep response) will then be used to refine constitutive models for subsequent numerical analyses and assess the results of those analyses. The analysis results will help define acceptable pressure load cycling rates and perhaps provide insight towards engineering guidelines for the operation/design of caverns for use in this high frequency manner.

This paper reports on the initial results from an *in progress* experimental program designed to study the effect of cyclic differential stress changes on the mechanical properties of rock salt. The differential stress regime was chosen to be relatively low in order to discover if small stress changes would have any impact on the mechanical properties of the rock salt.

If cavern pressurizations/depressurizations are to be used in a manner to load-follow a renewable in situations described above in an unbuffered manner (buffering may be achieved with another smaller capacity energy storage medium), changes in cavern pressure could be abrupt and repetitious. If a cavern were to be operated at a relatively high average pressure (for example 60% to 90% of the casing shoe pressure) the salt stress state condition should remain in a non-dilatational state. Our desire was to evaluate the scenario wherein rock salt was subjected to cyclic loads at differential stresses below the short term dilation stress state.

The effect of cyclic loading on the elasticity and strengths of geologic materials has long been recognized (for example, Haimson, 1974). Cyclic loading coupled with time-dependent deformation of a semi-brittle material like salt has also been studied experimentally, (for example: Thoms and Gehle, 1982; Matei and Cristescu, 2000; Allemadou and Dusseault, 1996; Bauer, et al, 2010; and Dusterloh and Lux, 2010 and other researchers).

In our previous work on cyclic loading of rock salt (Bauer et al, 2010) we observed changes in volume strain and Young’s modulus, observed but did not quantify microcracks in thick sections, and detected acoustic emissions. These results were consistent with previous work and implied that cyclic loading caused cracking at low differential stresses. This work intends to extend the results of these previous studies.

Experimental Approach

A Gulf Coast domal salt, (approximately 98% halite) was used in this study. The crystal size ranges from about ¼” to ½” and the rock salt has a density of about 2.15-2.16 g/cc; the average UCS for this rock salt is approximately 3500 psi. Room dry specimens were first mechanically characterized for its dilation “strength” response (Figure 1) through a series of triaxial compression tests over a range of confining pressures. The dilation strength was determined as the stress state at which a change in direction of the volume strain versus differential stress curve was observed wherein the behavior changes from compaction to dilation. A curve was fit to these experimental data. Using this empirical curve as a guide, and selecting (for this test series) 3000 psi as a confining pressure, stress states appropriate to 50% and 60% of the differential stress dilation “strength” were determined (Figure 1).

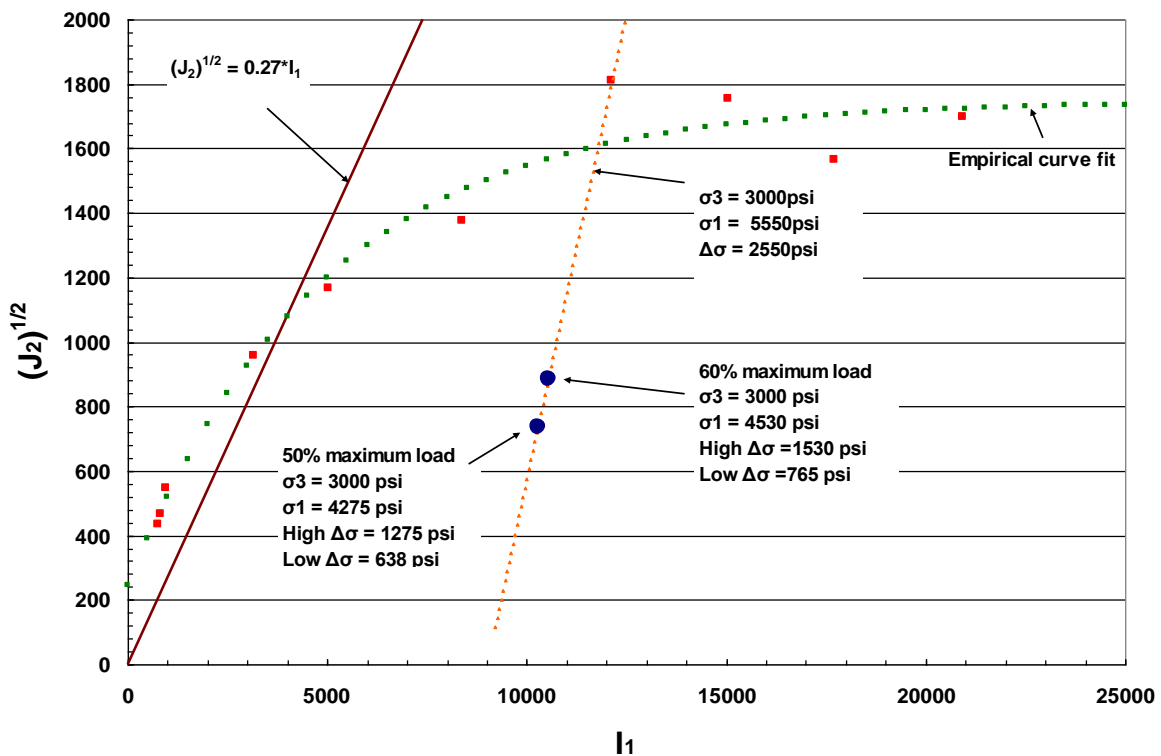


Figure 1. Dilatant behavior of salt determined from quasi-static tests and stress states for tests conducted as part of this study.

Using this mechanical characterization, stress state cycling limits were chosen to test the salt. Then, room dry and oven dried specimens of field core (end prepped right circular cylinders nominally 4" in diameter and 8" long, specimens are not annealed prior to testing) were confined at 3000 psi for 24 hours and were cycled (in triaxial compression) between 25-30% and 50-60% of the dilatant strength. Specimens were cycled up, held at constant stress for ~ 160 minutes, then cycled down, and then again held for ~ 160 minutes. Specimens experienced about four load cycles per day; tests ran from 12 days to about 60 days, resulting in about 40 to 240 load cycles on different specimens. The load cycles are intended to be used to elucidate potential effects of load cycling of salt at confining pressure. The load cycles are not intended to represent load cycles imposed by renewable energy storage operations.

Each cyclic test specimen was ramped up at ~1.8 psi/sec loading rate to the desired upper load. (Specimens were in load control). Specimens were then held at the constant differential stress for approximately 160 minutes, and then unloaded at ~1.8 psi/sec unloading rate to the desired lower differential stress and held there for approximately 160 minutes. The aforementioned loading/unloading rate corresponds to an approximate axial strain rate of $3.6 \times 10^{-7} \text{ s}^{-1}$. Data were collected every 120 seconds during the "hold" portions of the test, and every 5 seconds during the load ramp periods; the 5 second data rates began one minute before initiating and after ending a ramp period. The load cycling was repeated for the duration of each experiment. Specimens were unloaded to hydrostatic, and subsequently returned to ambient pressure. During each experiment, axial force and axial displacements were recorded; for tests 3 and 4 radial displacements were recorded as well. In test 4, acoustic emissions were recorded for a portion of the test. In test 5, acoustic emissions were recorded for most of the test. Thus far, five experiments have been completed ranging from 12 to 62 days duration (Table 1). Tests 1 and 2 specimens were room dry. Tests 3, 4, and 5 specimens were oven dried for 24 hours at 100°C. The water content of all test specimens is unknown, but domal salts are generally dry.

Table 1. Test matrix for cyclic tests

Test #	dryness	$\Delta\sigma_D$ max (psi)	$\Delta\sigma_D$ min (psi)	Duration (days)	E_i (msi)	E_{max} (msi)	E_{min} (msi)
1	room	1596	800	61.9	4.85	5.02	3.92
2	room	1273	637	12.0	4.87	4.90	4.41
3	dried at 100°C	1275	638	32.0	4.87	5.10	3.95
4	dried at 100°C	1532	770	22.9	4.58	4.71	4.36
5	dried at 100°C	1400	700	18.8	5.04	5.37	4.95

The computer-controlled servohydraulic testing system used to conduct the room-temperature (77°F) quasi-static triaxial compression tests on the domal rock salt specimens described in Table 1 is shown in Figure 2. The system is comprised of an SBEL pressure vessel assembly and an MTS Systems reaction frame. During testing, the pressure vessel housing the test specimen was hydraulically connected to a pressure intensifier capable of inducing pressures up to 30,000 psi using Isopar® as the pressurizing medium. The reaction frame is equipped with a moveable cross-head to accommodate various sizes of pressure vessel assemblies and is capable of applying axial loads up to 220,000 pounds through a hydraulic actuator located in the base of the frame. Vessel pressures were measured by a pressure transducer plumbed directly into the hard line that supplies the pressure to the vessel. It is located ~ 4 ft. from the pressure vessel. Axial loads were measured by a load cell located outside the pressure vessel.

Each test specimen was jacketed in a ~1/16-inch-thick impervious heat shrink membrane to prevent the confining pressure fluid from contacting and/or entering the accessible pore space of the specimen when it was placed under pressure in the pressure vessel. Jacketing represents a mechanical boundary unlike a CAES cavern boundary where the pore pressure of the damaged salt can change in response to pressure changes in the cavern.

The jackets were sealed to hardened steel end caps above and below the specimen with 304 stainless steel wire. The ends of the specimens are lubricated to the end caps with a 50:50 mixture of petroleum jelly and stearic acid (Labuz and Brindell,1993).

Test specimens were instrumented with electronic deformation transducers before they were placed in the pressure vessel assembly. Radial deformation was measured using two linear variable differential transformers (LVDTs) oriented at 90° to each other near the specimen mid height. Axial deformation was measured by two LVDTs mounted to the specimen endcaps (Figure 3). Displacement measurements are averaged for strain calculations. During unload cycles, the axial stress versus strain response permitted determination of Young's modulus.



Figure 2. Testing system used to conduct cyclic load triaxial compression tests.

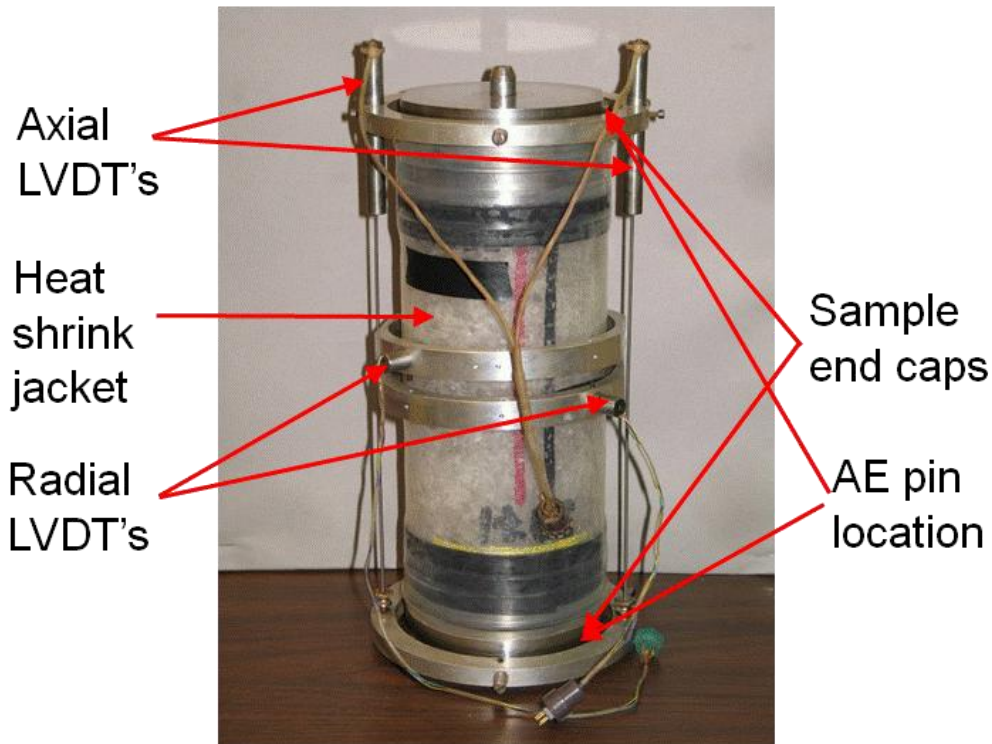


Figure 3. Specimen assembly

Setup of the quasi-static triaxial compression tests included placing the jacketed, instrumented specimen assembly into the pressure vessel, connecting instrumentation leads to feed-throughs in the pressure vessel and mounting the pressure vessel assembly into the reaction frame (Figure 2). The actuator in the base of the frame was then advanced gradually, raising the pressure vessel assembly into position for the test. A small axial preload was applied to the specimen through a push-rod that extended through the top of the pressure vessel and was in direct contact with the crosshead load cell on one end and the specimen on the other. Then, initiation of the test was turned over to the test system controllers which automatically increased the confining pressure and axial stress to ensure the specimen was loaded to the correct hydrostatic confining stress. Once the test system had stabilized at the target pressure for 24 hours, the cyclic loading portion of the test was initiated. (Note: Test 1 was subjected to extended time periods of high and low “holds” early in the test, while we were developing the experimental method; Test 4 was overloaded by about 70 psi at the start of the test for about 700 seconds).

Three quasi-static constant strain rate tests were first completed to improve our understanding of the workings of the acoustic emission system. The three tests, each run at 2000 psi confining pressure, and different strain rates (3.3 hr, 36 hr, and 97 hr duration tests). The tests were completed on 4 inch diameter and 8 inch long domal salt specimens to provide insight into a strain rate effect upon the acoustic emission response.

Following the constant strain rate test series, we began a constant mean stress test series, to evaluate acoustic emission response in the CMS loading mode, completed on domal salt specimens from a different salt dome.

Acoustic emissions are produced by rapid microcrack growth and are associated with brittle fracture. Counting of the number of AE events prior to failure has shown a correlation between AE rate and the inelastic strain rate (Lockner, 1993). In this study we have begun to make such correlations in tests of semi-brittle deformation of rock salt in constant strain rate, constant mean stress, and cyclic loading.

Acoustic Emission System

The premise of seeking to detect acoustic emissions is simple. As the rock is deformed, grains will debond and crush against one another generating acoustic waves (sound). The acoustic wave then travels omnidirectionally through the material, where it is sensed and recorded by an appropriate device. The sensing devices used in this work are piezoelectric event arrival pins. The pins sense the wave and convert it to an analog electrical signal to be recorded after further processing by the rest of the AE system.

The acoustic emission system in use in this work is a passive sampling system, meaning that it only detects events naturally occurring within the specimen. Once an event occurs within the specimen the acoustic emission system amplifies it through a 60 db amplifier, bringing the signal up to the 20-50 mV range. This higher voltage range makes it easier to discriminate the events and subsequently record the event with the high-speed digitizers (capable of sampling at 40MHz) attached to a nearby computer. The discriminator compares signals on multiple pins to determine if an event actually occurred.

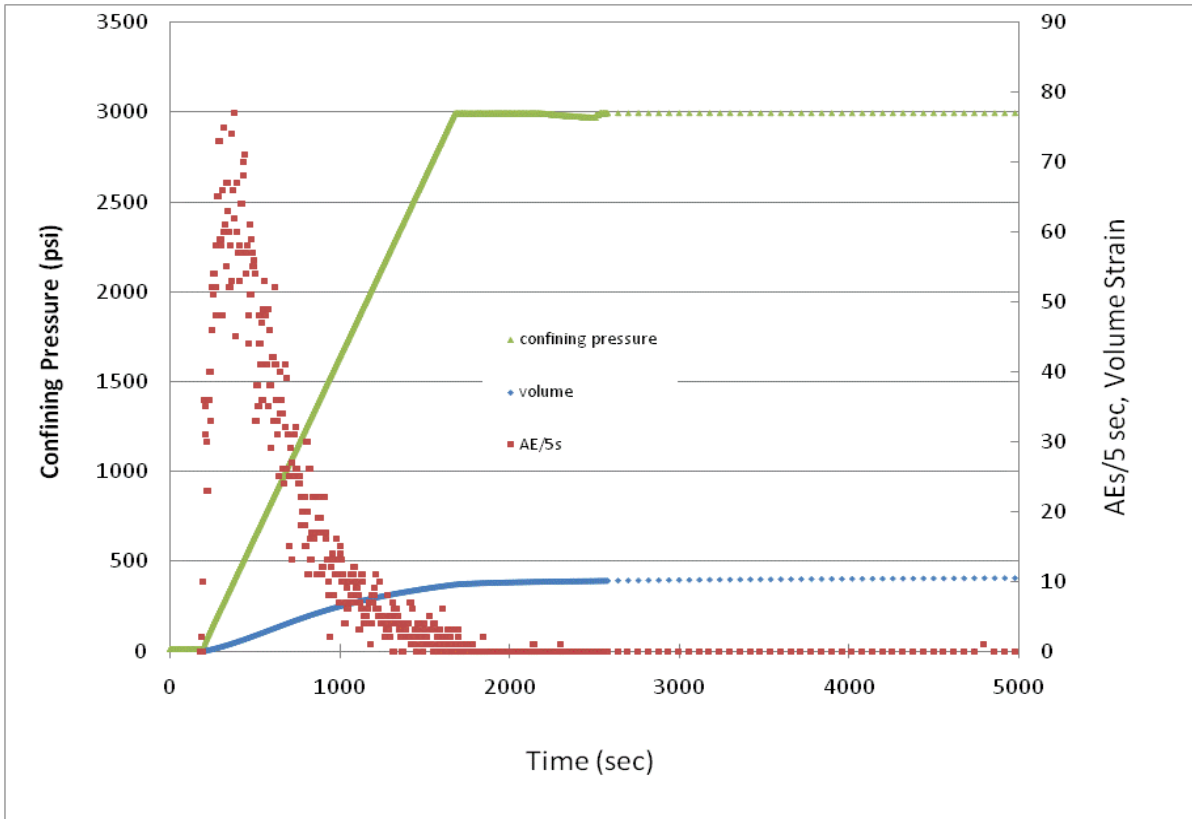
In our tests, there was either one pin attached to one end cap, or one pin on each end cap. While this placement is not ideal it is sufficient for the purposes of this work. Ideally the pins should be attached directly to the specimen. The discriminator was set to trigger on one or two signals respectively. After the test is complete these data are analyzed for number of events per unit of time.

Results

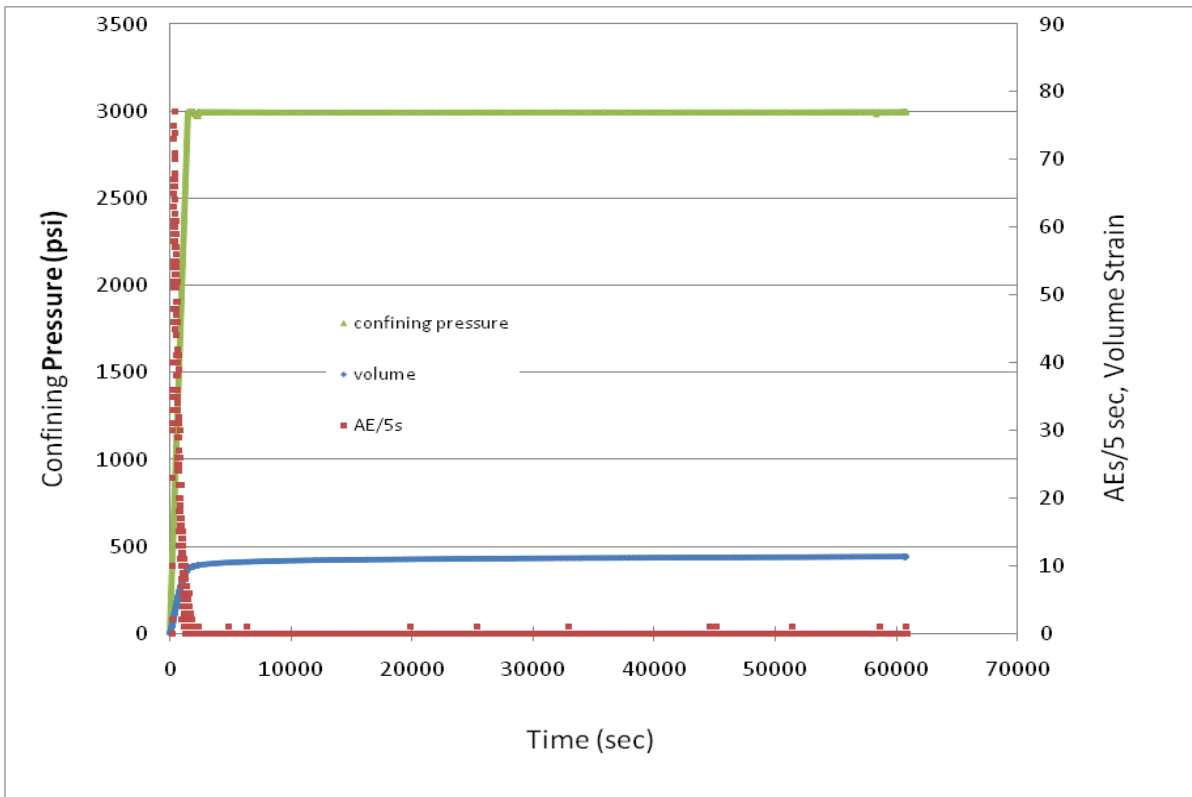
The results presented show the occurrence of AEs in different stress states, namely application of confining pressure, application of differential stress at a constant confining pressure, constant means stress testing and cyclic load testing at constant confining pressure.

Application of Confining Pressure

Upon increasing confining pressure the volume is observed to decrease (Figure 4). The volume continues to decrease after reaching the test pressure (here 3000 psi) and for more than 16 hours of pressure soak. This implies that there was some loosening of the grain boundaries induced during the field coring process. During the early application of confining pressure, AE events are observed, but they begin to diminish in number after about 1000 psi confining pressure has been reached, but they do continue to occur for the entire pressurization (Figure 4a), and in some numbers for a short time after the peak pressure is reached. AE events generally fall to zero after about 2000 seconds test time, but occasionally occur for the entire 16+ hour confining pressure only portion of the test. Volume strain (here multiplied by 1000 for it to be plotted on this scale) has its largest change during pressurization, and it continues to compress at a minimal and decreasing rate for the entire 16+ hour confining pressure only portion of the test. The AE and volume strain data taken together imply that much of the volume closure observed during the pressurization occurs via audible crack closure and slippage. After about 2000 seconds, volume closure continues to a very small degree and near inaudible manner. One may conclude that this further closure is accomplished by intragranular deformation adjacent to/ in the vicinity of cracks.



4a

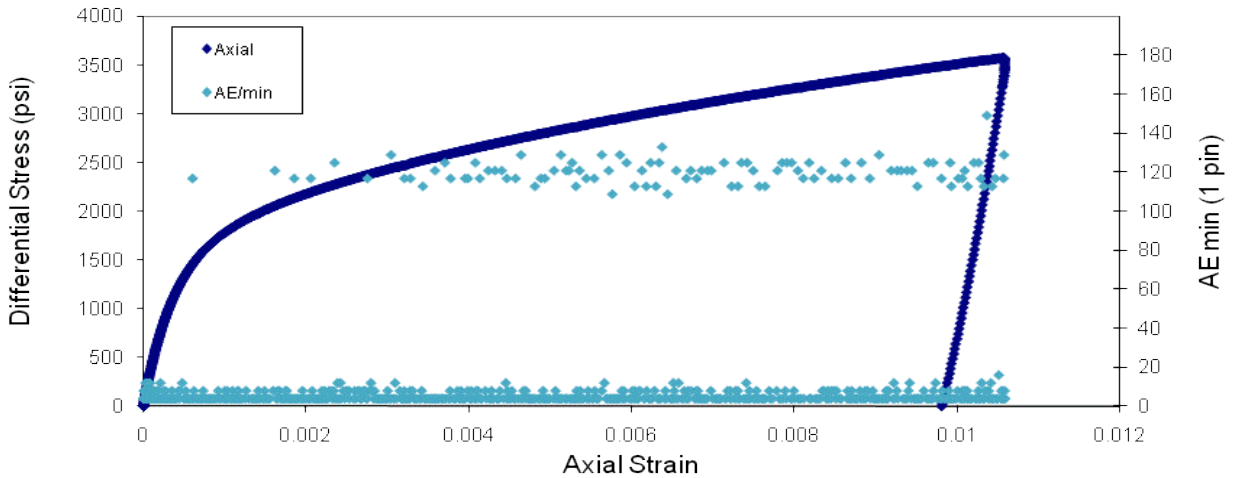


4b

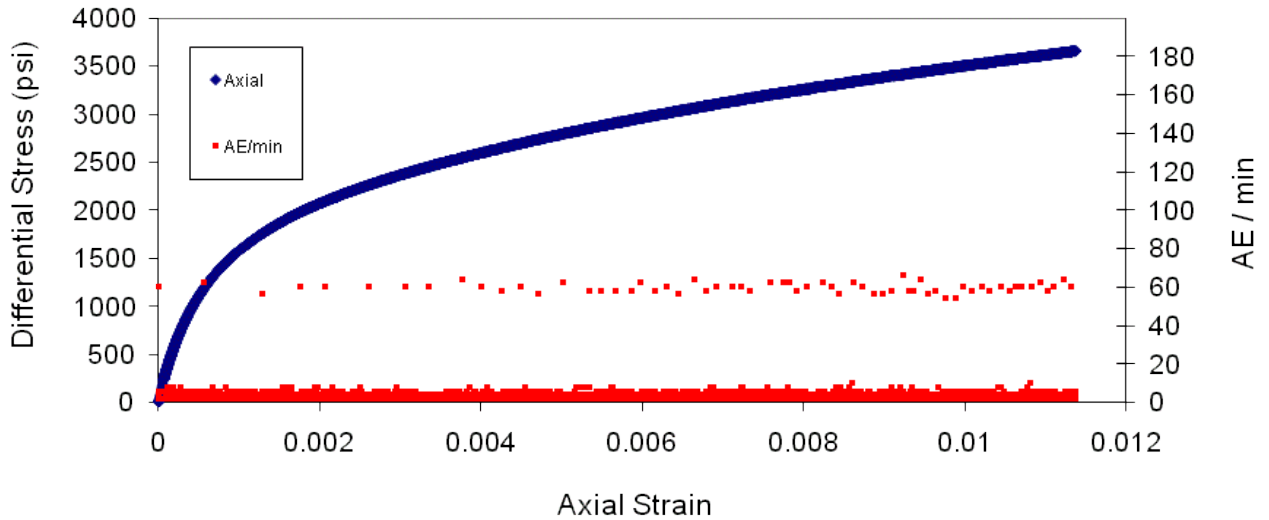
Figure 4. Confining pressure, volume strain, and acoustic emissions/5sec (a: early test; b: all of confining pressure only application).

Constant strain rate and strain rate effects

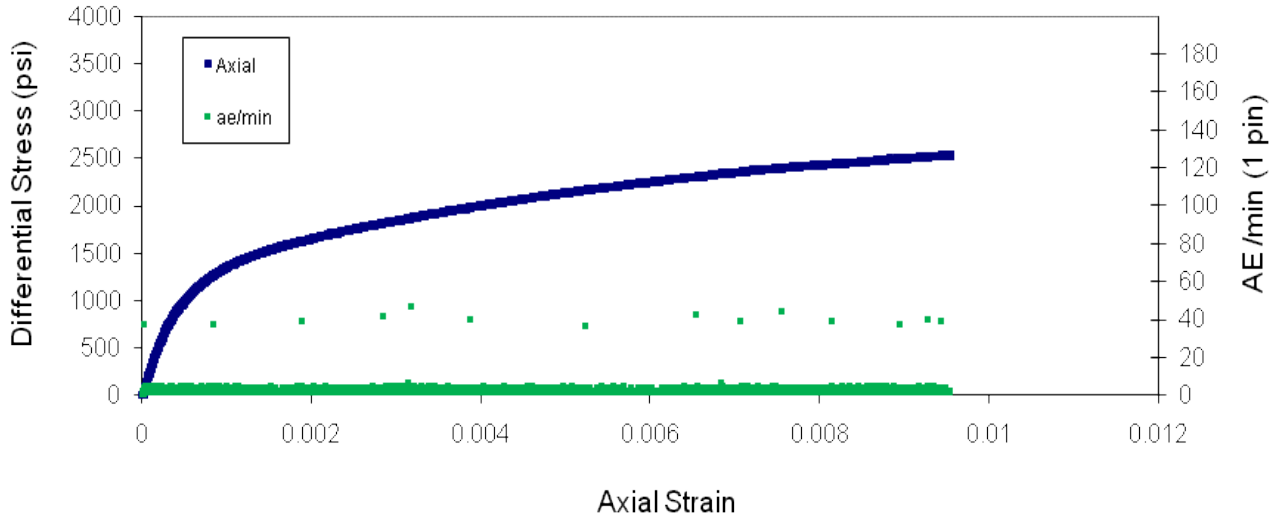
In this section three quasistatic constant strain rate tests conducted at 2000 psi confining pressure are discussed, ranging in test time from 3.3 hours to over 97 hours to achieve about 1% axial strain. The AE data in this section were obtained with a single pin. For all tests (and strain rates) a few AEs are observed during the early portion of the test; once the specimen appears to yield, many more AEs occur (Figure 5 a-c). For all tests there is a persistent low level background of AEs throughout the tests. It appears that the event rate increases with increasing strain for a given test. It also appears that the greater the strain rate, the greater the number of AEs. This is consistent with faster strain rates promoting brittle processes (microfracturing), and slower strain rates promoting ductile process (intragranular flow) together with microfracture to accommodate strain.



A: test time =3.3 hr



B: test time =36 hr



C: test time =97 hr

Figure 5. Differential stress, AEs/min versus Axial Strain

Constant mean stress testing

In this test series we present the (test results are represented by only one test) observations of AE data collected in conjunction with constant mean stress testing. In this type of test, the specimen is first subjected to confining pressure (for this test 3000 psi), and then the axial stress is increased at the same time the confining pressure (representing the minimum and intermediate stress) is decreased at a rate to maintain a constant mean stress.

The results of such a test are presented in Figure 6 wherein axial and volume strain and AEs are plotted against differential stress. AEs begin to increase from the start of the test and acquire a high rate that is maintained once the specimen has yielded.

In comparing AEs to volume strain (Figure 7), AEs occur during initial volume decrease (compaction), representing crack closure, slippage, and initiation. Once the specimen begins to dilate, when crack initiation and growth is more prevalent, a greater number of AEs occur. AE rates are near constant and high for ever increasing volume strains during the deformation.

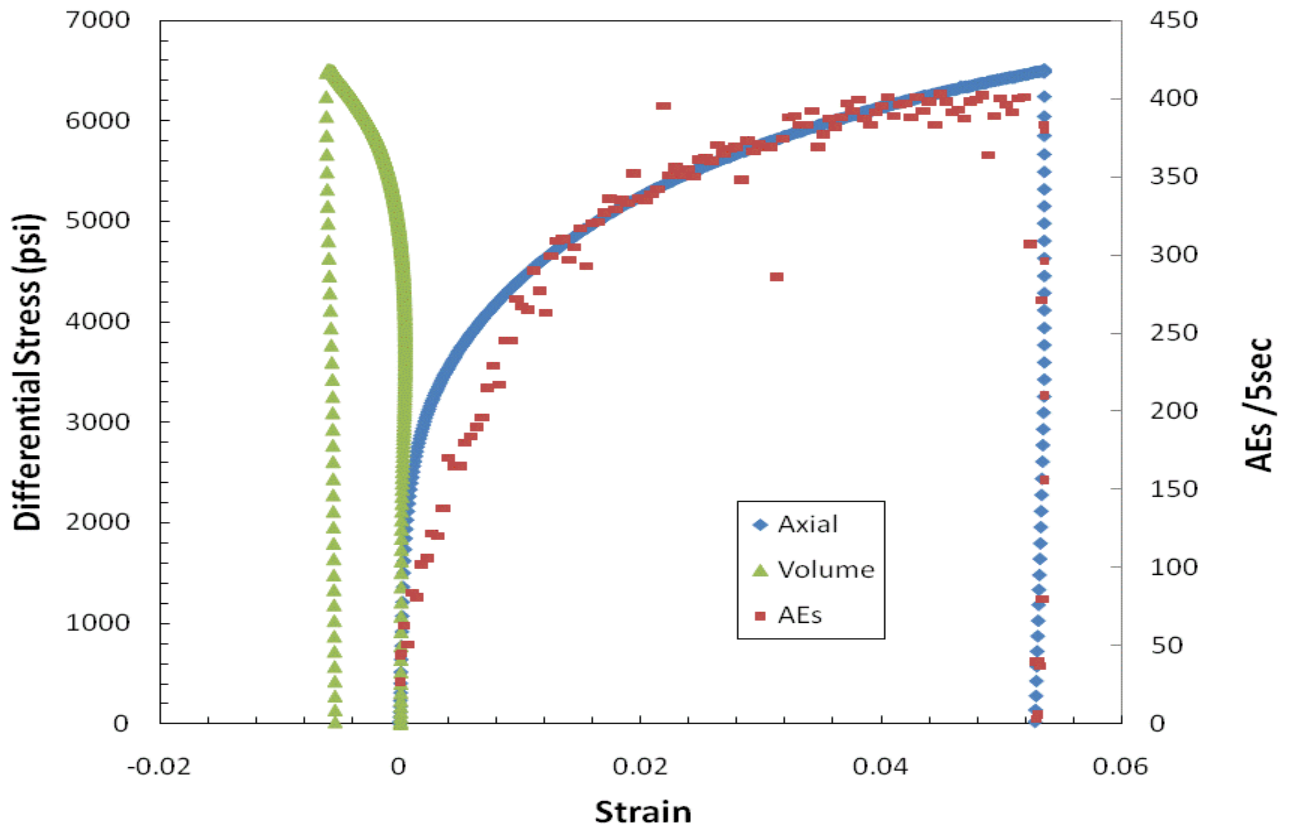


Figure 6. Axial and volume strain and AEs/5 sec versus differential stress for constant mean stress loading.

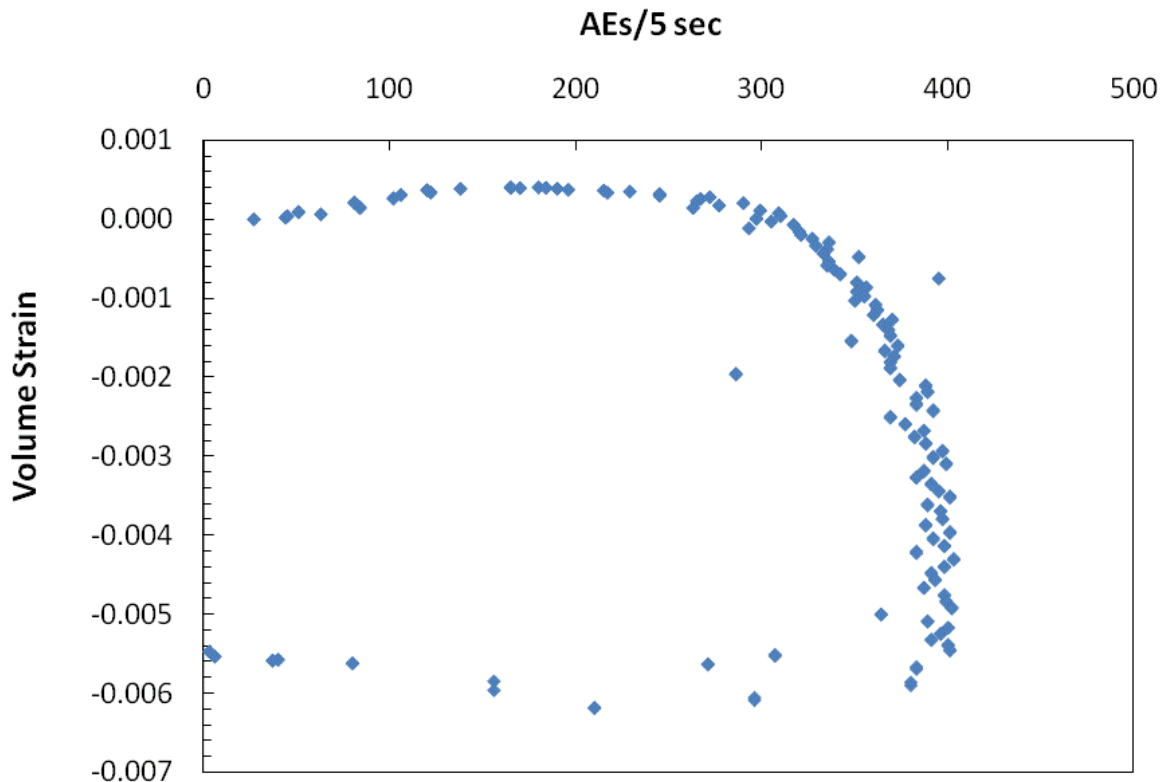


Figure 7. Volume strain versus AEs/5 sec for constant mean stress loading.

Cyclic Testing

One additional experiment, cyclically loaded in triaxial compression at 3000 psi confining pressure, differential stress cycles of 700 and 1400 psi and instrumented with two AE transducers, was completed. The test ran for approximately 18.8 days. Results are presented as percent axial strain and acoustic emissions versus time (Figure 8). Acoustic emissions are plotted here as events/4 minutes and are observed throughout the test.

In Figures 9, 10, and 11 the test results are plotted at a greater scale for the beginning, middle, and end of the test, respectively. Each upper (differential stress = 1400 psi) constant stress hold period and lower (differential stress = 700 psi) constant stress hold period is represented by creep strain in the specimen. For all test times, the creep strain at the upper load level increases with increasing time, however the rate at which the strain increases decreases with increasing time. For all test times, the creep strain at the lower load level decreases (recovers) with increasing time, with what appears to be at a decreasing strain rate with increasing time.

The data have not yet been sufficiently scrutinized to determine a correlation between acoustic emission numbers and strain. This work is ongoing. This test was not taken to a point where the specimen reversed its volume strain. The Young's modulus calculated as a function of time/strain for this test remained about the same for the entire test, implying this specimen tested at this stress level did not reach a condition where volume increase occurred (this is different than our previous work, but only means that this specimen, although loaded to similar stress states as in our previous work, began as an inherently stronger specimen than some of the specimens used in our previous work [i.e. specimen to specimen variability]).

(Note; there are bare segments in the data; these represent times when the AE system was borrowed for other testing. Also, some of the hummocks in the data are caused by minor fluctuations in lab temperature effecting electronic conditioning.)

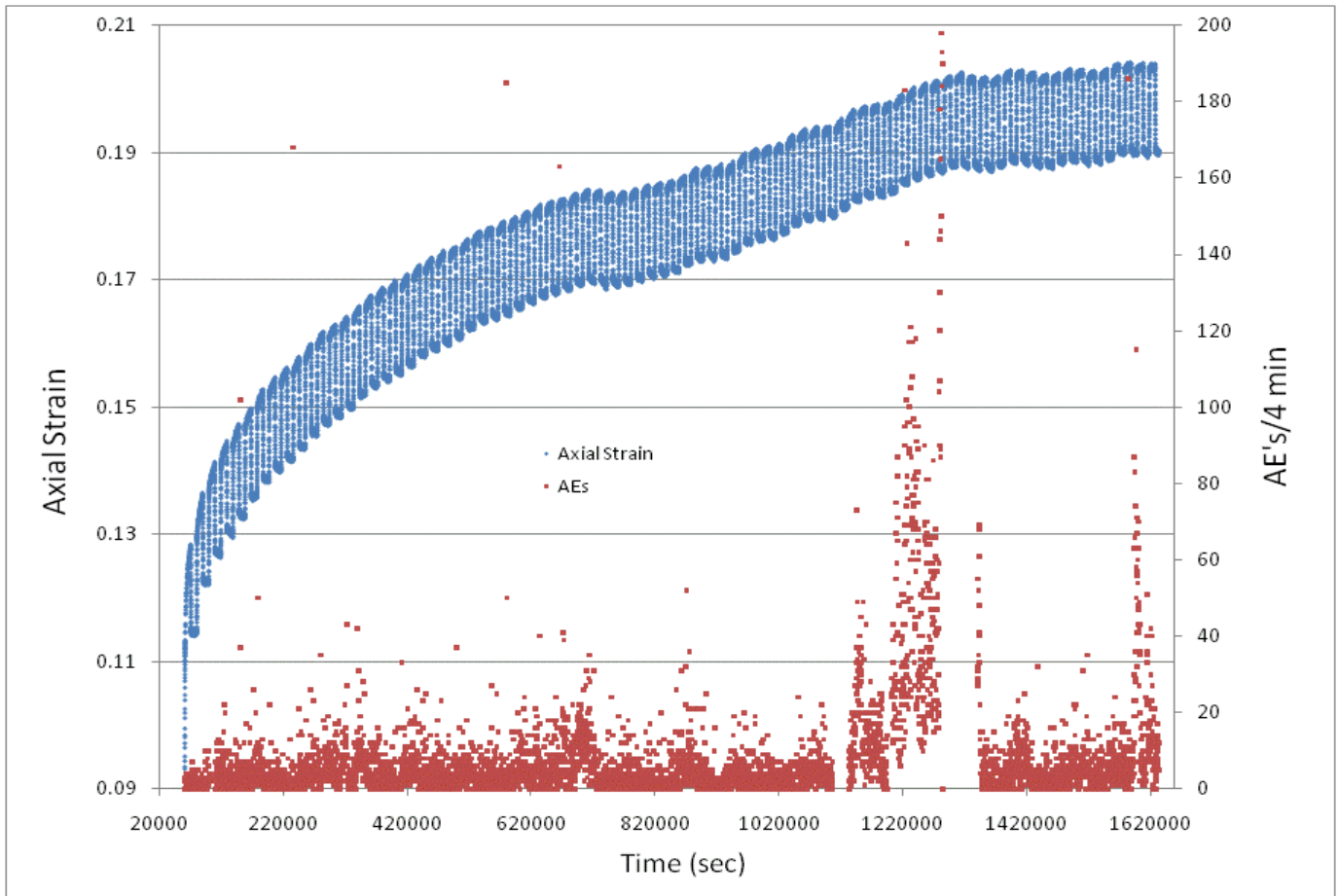


Figure 8. Axial Strain and acoustic emissions versus time.

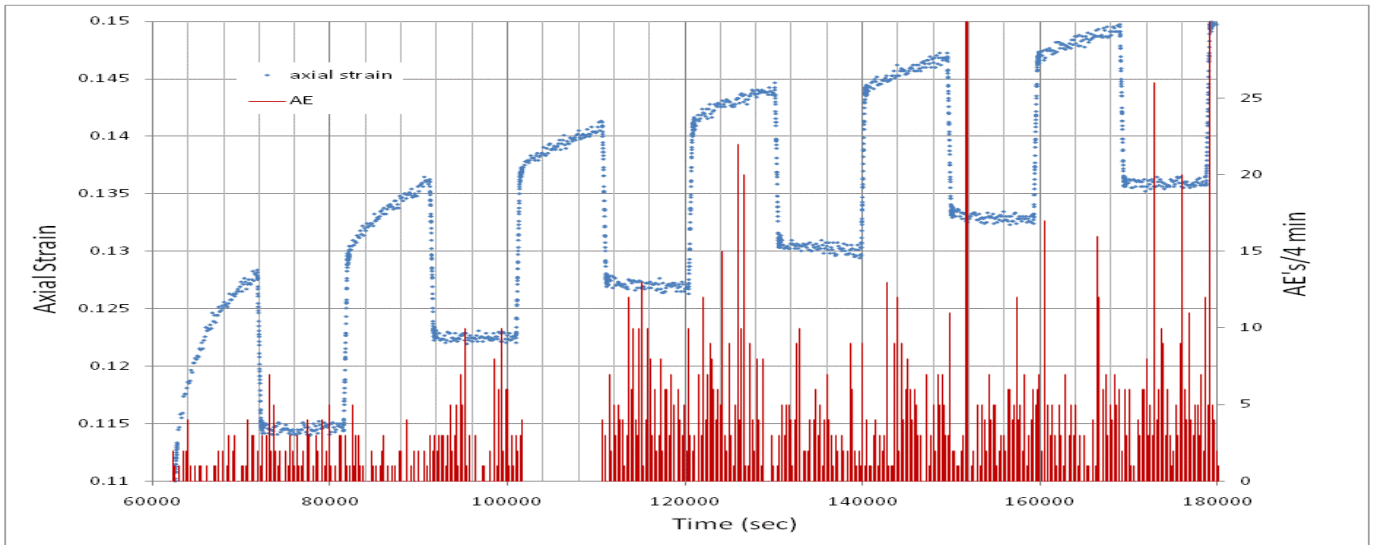


Figure 9. Percent axial strain and acoustic emissions versus time, early test.

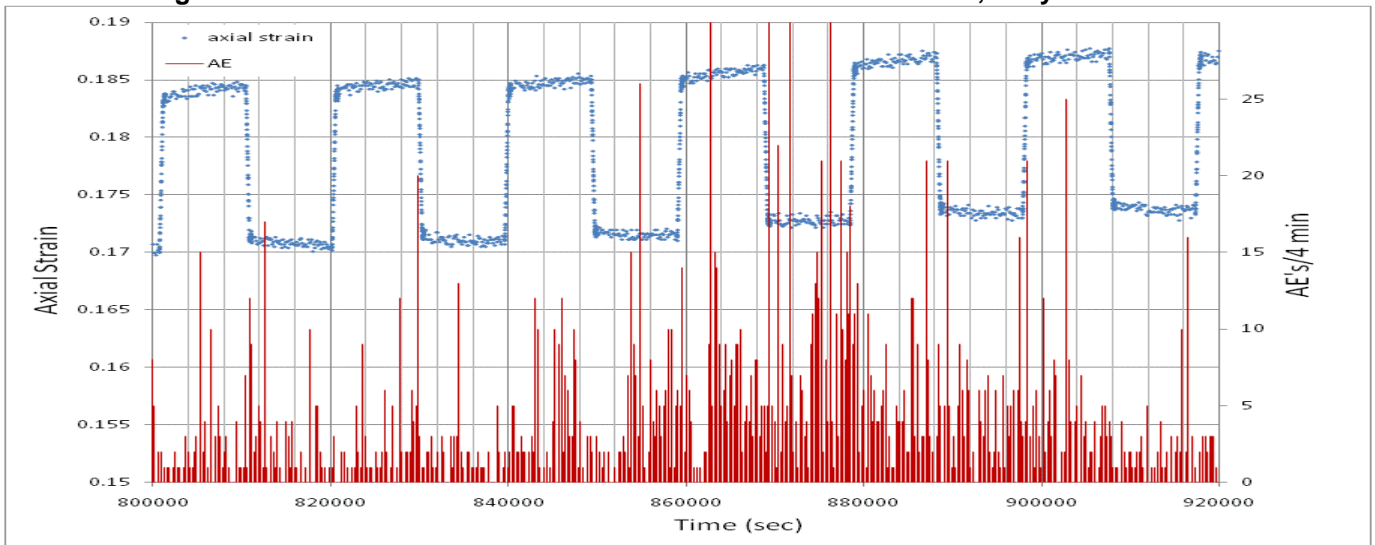


Figure 10. Percent axial strain and acoustic emissions versus time, mid test.

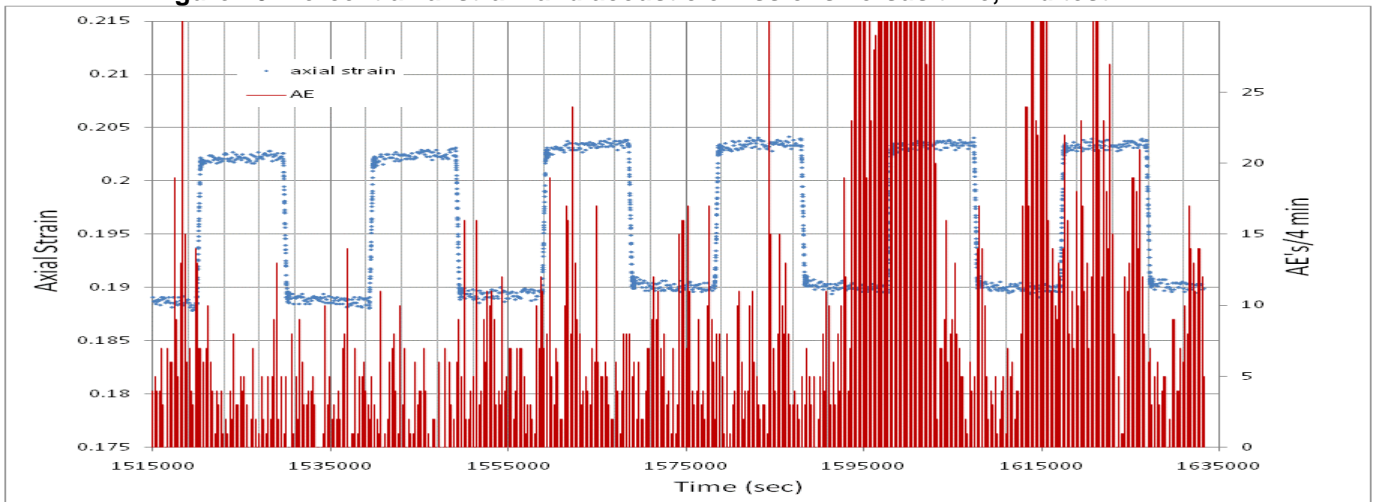


Figure 11. Percent axial strain and acoustic emissions versus time, end test.

Summary, Discussion, Comments, Conclusions

We have presented results of confined triaxial compression tests on a domal salt; constant strain rate, constant mean stress, and cyclic loading tests. The results of this work document certain aspects of semi-brittle deformation of rock salt, which has been studied extensively in the brittle (e.g. Hansen and Fossum, 1986) and ductile (e.g. Carter and Hansen, 1983) regimes. The objective of this work was to obtain a better understanding of our previous experimental results (Bauer et al, 2010), and that of others, through the use of acoustic emissions. In our previous work we observed changes in volume strain and Young's modulus, observed microfractures in thick optical sections, and detected acoustic emissions; these results were consistent with the work of others in similar testing and implied that cyclic loading caused cracking at low differential stresses, below the short term dilatancy boundary.

In our previous work on cyclic loading of salt we offered a mechanistic explanation of our results, considering that a polycrystalline salt aggregate is being deformed. At room temperature and 3000 psi confining pressure, both plastic and brittle deformation mechanisms are operative. The co-operation of the two sets of deformation mechanisms leads to microcracking at low stress levels. The inclusion of acoustic emission to the data collection has extended our knowledge and improved confidence in our interpretation by giving an indication of when brittle processes are operative during imposed deformation conditions.

Upon application of confining pressure, rock specimens compress due to crack closure. The compression is both fast (tracking the increase in confining pressure) and time dependent. This experimental observation is consistent with that of Brodsky (1990) who measured volume strain and velocity changes, and Allemandou and Dusseault, (1993) and De Vries and Mellegard (2010). Acoustic emission activity is observed early in our tests and diminishes to near zero shortly after the confining pressure maximum is reached. The AE and volume strain data taken together imply that much of the volume closure observed during the pressurization occurs via audible crack closure and slippage. After full pressurization, volume closure continues at a minimal rate and in a near inaudible manner. This continued compaction and crack closure is accomplished by intragranular deformation adjacent to/in the vicinity of cracks. The interpretation of the combination of brittle and plastic deformation mechanisms to accommodate crack closure is consistent with Brodsky (1990).

In the constant strain rate tests, only a few counts are observed during the early loading in the tests. Once the specimen yields, many more counts occur; it appears that the count rate increases with increasing strain for a given test. The greater the strain rate, the greater the number of counts. Greater strain rates promote brittle processes (microfracturing), and slower strain rate promote ductile process (intragranular flow) to accommodate strain.

In constant mean stress testing, acoustic emissions begin to increase from the start of the test and acquire a high rate that is maintained once the specimen has yielded. AEs occur during initial volume decrease (compaction), representing crack closure, slippage, and initiation. Once the specimen begins to dilate, when crack initiation and growth is more prevalent, a greater number of AEs occur. AE rates are near constant and high for ever increasing volume strains during the deformation. It is interesting to note that permeability of damaged salt also steeply increases by several orders of magnitude during the small initial volumetric strain, and thereafter levels off in a manner qualitatively represented by the AE data. As it turns out, the initial fractures continue to expand such that the total volumetric strain of the sample results from a few larger fractures parallel to the maximum principal stress. (Pfeifle, et al 1998, Stormont, 1990)

The cyclic test performed coupled with acoustic emission data allow us to more confidently conclude that microcracking is occurring in this test, as well as tests performed previously (Bauer et al 2010). The occurrence of microcracking was concluded through the observed reversal in volume strain and decrease in modulus (Bauer, et al 2010). The dilatant behavior was observed well below (50-60%) the short term experimental dilatancy envelope.

Early in the tests the changes in Young's modulus reflect hardening or compression of the material. Compression corresponds to closure of pre-existent microfractures. Hardening suggests dislocations have moved to pileup positions. Either or both of the mechanisms are possible. At room temperature one may not expect a great deal of climb to relieve pileups. During continued cycles of deformation, dislocations are continually pushed to pile up positions, and at times locked into these positions. Load cycling eventually leads to microcrack formation, apparently at each load cycle because grain scale load and unload paths are

not coincident even though much of the stored strain energy is “elastic”. Microcracks are closed and opened, perhaps, at each load cycle. The deformation process may be systematic, but depends on local crystallographic orientation relative to the locally imposed stress and strain field in the polycrystalline aggregate, thus the manifested deformation is locally abrupt in terms of cracks forming, but perhaps less abrupt and/or gradual in terms of the time/strain based changes in modulus observed. This explanation is consistent with the small oscillatory transition in volumetric strain observed and the acoustic emissions recorded, and the observed (but not as yet quantified) presence of microcracks.

The semi-brittle deformation observed is consistent with the work of Fuenkajorn and Phueakphum (2009) and Matei and Cristescu (2000), and others not cited. Shortcomings of our work include the fact that although we used, for each experiment, the same rock salt, each had different “starting” microstructures. This could have influenced the results. Also, no measures to “anneal” the specimens, or condition them other than an overnight hold at confining pressure as has been recommended (Allemadou and Dusseault, 1993) were employed. The presence of pre-existing cracks in an unknown way most likely affected the measured results within each specimen, and is likely a cause of specimen to specimen test result variability. Finally, the displacements/strains recorded during these tests are small, however the experimental results are somewhat consistent/repeatable from test to test. The results are consistent with evaluating similar phenomena identified by previous workers using different approaches, and the measurement magnitudes are similar to those of previous researchers (for example, Allemadou and Dusseault, 1993).

The results of this work **do not** necessarily imply that salt caverns when cyclically loaded will progressively deform to macroscopic failure. The results do demonstrate that cyclic loading causes dilatant behavior at stress levels below the short term dilatancy envelope. How this is manifested at the cavern scale has yet to be determined. Increased confining pressure, increased temperature, and decreased strain rate (studied in this paper) will act to suppress microfracturing; conditions that suppress microfracturing improve with distance into the cavern wall.

We note that jacketing of test specimens represents a mechanical boundary unlike a CAES cavern boundary where the pore pressure of the salt can change in response to pressure changes in the cavern.

Munson, et al (1998), discuss interior cavern conditions and salt fall potential. Their work focuses on creep fracture and does not address cyclic loading, but some of the results are applicable here. They observe that the accumulation of fallen salt generally increases with increasing impurity content. They also conclude that fallen pieces of salt must be “small” because large pieces of fallen salt would cause casing damage (which does happen sometimes). Munson, et al also point out that conditions for salt fracture are at or near the cavern wall and that away from the wall, into the rib confining pressure increases and fracture is suppressed.

The use of acoustic emissions as diagnostics for rock salt deformation has been studied in the laboratory. This technique could be applied to cavern scale monitoring; cemented casings for caverns extend to the cavern shoe. A transducer/monitoring device could be affixed to surface piping to listen to subsurface noise and rate or pattern of acoustic events; this might be used to assess progressive subsurface damage.

This work provides an evaluation of the Kaiser effect in rock salt. For many rocks it is observed that acoustic emissions due to microcracking are detected only during the first loading in compression to a given stress state. If that first loading/stress state is subsequently exceeded AEs will again be observed (Holcomb 1985, Li and Nordlund, 1993). Here we observed AEs at both the upper and lower stress levels throughout the cyclic test. It appears that the combination of brittle and ductile process facilitates local stress/strain relaxations such that microcracks can open or close upon **each** loading and unloading so the Kaiser effect is not observed.

An implication may be that the dilatancy criteria used to determine operational limits of salt caverns should be revisited, especially if salt caverns will be used to support renewable energy resources. If salt strengths are lowered due to frequent small pressure change cycling, this could be detrimental to cavern longevity. Perhaps operational characteristics of such caverns need be adjusted to allow for crack healing. It is likely elevated temperatures commensurate with the geologic thermal gradients, and or ground warming due to gas compression, will activate more ductile deformation mechanisms and brittle processes will be eschewed.

Bibliography

- Allemandou, X., and M. Dusseault, 1993, Procedures for cyclic creep testing of salt rock, results and discussions. Proceedings of the 3rd Conference on the Mechanical Behavior of Salt; Sept 14-16, 1993; Clausthal-Zellerfeld, Trans Tech Publications, p. 207-218.
- Bauer, S., S. Broome, and D. Bronowski, 2010, Experimental Deformation of Salt in Cyclic Loading SMRI Spring 2010 Technical Conference, April 2010, Grand Junction, CO, USA
- Brodsky, N.S., 1990, Crack Closure and Healing Studies in WIPP Salt Using Compressional Wave Velocity and Attenuation Measurements: Test Methods and Results, SAND90-7076, Sandia National Laboratories, Albuquerque, NM, 87123
- Carter, N.L., and F. D. Hansen, 1983, Creep of Rocksalt, *Tectonophysics*, V. 92, 1/4, 1 pp 275-333.
- DeVries, K., and K. Mellegard, 2010, Effect of Specimen Preconditioning on Salt Dilation Onset, SMRI Fall 2010 Technical Conference, 3–6 October 2010, Leipzig, Germany
- Düsterloh, U. and K.-H. Lux, 2010, Some geomechanical aspects of compressed air energy storage (CAES) in salt caverns, SMRI Fall 2010 Technical Conference, 3–6 October 2010, Leipzig, Germany
- Fuenkajorn, K. and D. Phueakphum, 2009, Effects of Cyclic Loading on the Mechanical Properties of Maha Sarakham Salt, *April, 2009 Suranaree J. Sci. Technol.* 16(2):91-102, Thailand.
- Haimson, B.C., 1974, Mechanical behavior of rock under cyclic loading. Proceedings of the 3rd Congress of the International Society for Rock Mechanics, Part A. Advances in Rock Mechanics: Report of Current Research; Sept 1-7, 1974; Denver, National Academy of Sciences, Washington, D.C., p. 373-387.
- Hansen, F.D., and A. Fossum, 1986, Failure of Salt by Fracture, TR RSI-0304, prepared for ONWI.
- Holcomb, D., 1985, Summary of discussions on behavior of solids with a system of cracks. In: Bazant, Z.P., *Mechanics of geomaterials: rocks, concretes, soils.* J. Wiley, New York, 571-573.
- Labuz, J., and J. Bridell, 1993, Reducing Frictional Constraint in Compression Testing through Lubrication, *Int. J. Rock Mech. Min. Sci & Geomech. Abstr.* Vol.30 No.4, pp 451-455.
- Li, C. and E. Nordlund, 1993, Experimental Verification of the Kaiser Effect in Rocks, *Rock Mechanics and Rock Engineering*, 26 (4), 333-351.
- Lockner, D. 1993, The Role of Acoustic Emission in the Study of Rock Fracture, *Int. J. Rock Mech. Min. Sci & Geomech. Abstr.* Vol.30 No.7, pp 883-899
- Matei, A. and N.D. Cristescu, 2000, The effect of volumetric strain on elastic parameters for rock salt, *Mechanics of Cohesive-Frictional Materials*, V5:113-124.
- Munson, D., M. Molecke, and R. Myers, 1998, Interior Cavern Conditions and Salt Fall potential, Proc. SMRI, Spring Mtg, 1998, El Paso.
- Pfeifle T.W., N.S. Brodsky, and D.E. Munson. 1998. "Experimental Determination of the Relationship Between Permeability and Microfracture-Induced Damage in Bedded Salt," Proceedings, 3rd North American Rock Mechanics Symposium, NARMS '98, Cancun, Mexico, June 3-5, 1998. Published in *Int. J. of Rock Mechanics and Mining Sciences & Geomechanics Abstracts*. V. 35, no. 4/5, Paper No. 042.
- Stormont, J. C. 1990. Gas Permeability Changes in rock Salt During Deformation. PhD Dissertation. Tucson. AZ. University of Arizona.
- Thoms, R.L. and R. Gehle, 1982, Experimental study of rock salt for compressed air energy storage. Proceedings ISRM Symposium on Rock Mechanics: Caverns and pressure Shafts; May 26-28, 1982; Aachen, Germany, Taylor & Francis Group, p. 991-1002.